Original Article

Modeling of Gamma Index for Prediction of Pretreatment Quality Assurance in Stereotactic Body Radiation Therapy of the Liver

Rose Kamal[1,2], Deepak Thaper[1,2], Gaganpreet Singh[3], Shambhavi Sharma[2], Navjeet[1,2], Arun Singh Oinam[4], Vivek Kumar[5]

[1]Department of Radiation Oncology, Amrita Institute of Medical Sciences and Research Centre, Faridabad, Haryana, [2]Department of Radiation Oncology, Institute of Liver and Biliary Sciences, New Delhi, [3]Department of Medical Physics, Apollo Proton Cancer Centre, Chennai, Tamil Nadu, [4]Department of Radiotherapy, Post Graduate Institute of Medical Education and Research, Regional Cancer Centre, [5]Centre for Medical Physics, Panjab University, Chandigarh, India

Abstract

Purpose: The purpose of this study was to develop a predictive model to evaluate pretreatment patient-specific quality assurance (QA) based on treatment planning parameters for stereotactic body radiation therapy (SBRT) for liver carcinoma. **Materials and Methods:** We retrospectively selected 180 cases of liver SBRT treated using the volumetric modulated arc therapy technique. Numerous parameters defining the plan complexity were calculated from the DICOM-RP (Radiotherapy Plan) file using an in-house program developed in MATLAB. Patient-specific QA was performed with global gamma evaluation criteria of 2%/2 mm and 3%/3 mm in a relative mode using the Octavius two-dimensional detector array. Various statistical tests and multivariate predictive models were evaluated. **Results:** The leaf speed (MI_{LS}) and planning target volume size showed the highest correlation with the gamma criteria of 2%/2 mm and 3%/3 mm ($P < 0.05$). Degree of modulation (DoM), MCS_{SPORT}, leaf speed (MI_{LS}), and gantry speed (MI_{GS}) were predictors of global gamma pass rate (GPR) for 2%/2 mm (G22), whereas DoM, MCS_{SPORT}, leaf speed (MI_{LS}) and robust decision making were predictors of the global GPR criterion of 3%/3 mm (G33). The variance inflation factor values of all predictors were <2, indicating that the data were not associated with each other. For the G22 prediction, the sensitivity and specificity of the model were 75.0% and 75.0%, respectively, whereas, for G33 prediction, the sensitivity and specificity of the model were 74.9% and 85.7%%, respectively. **Conclusions:** The model was potentially beneficial as an easy alternative to pretreatment QA in predicting the uncertainty in plan deliverability at the planning stage and could help reduce resources in busy clinics.

Keywords: Gamma pass rate, hepatocellular carcinoma, modeling, pretreatment quality assurance, stereotactic body radiation therapy, volumetric modulated arc therapy

Received on: 19-12-2023 **Review completed on: 29-03-2024** **Accepted on: 09-04-2024** **Published on: 25-06-2024**

Introduction

Stereotactic body radiation therapy (SBRT) is commonly used for the treatment of liver cancers, where a high dose is delivered in a few fractions in contrast to conventional radiation treatments. Thus far, SBRT has shown promising results in the treatment of hepatocellular carcinoma (HCC).[1] Currently, volumetric modulated arc therapy (VMAT) with image guidance is a better delivery technique for SBRT than the modified dynamic conformal arc.[2] VMAT is a novel technique in which nonuniformity of the fluence is achieved by varying the gantry speed, dose rate (DR), and multileaf collimator (MLC) movements.[3] The total treatment delivery time is generally less in VMAT compared to intensity-modulated radiation therapy (IMRT) due to the treatment delivery using multiple static fields (five or more) in IMRT, and as a result, the probability of intra-fractional errors is also low.[4] The process of modulating the fluence using the aforementioned parameters increases the treatment plan complexity. Hence, uncertainty in treatment delivery is also increased. The uncertainties in dose delivery can be attributed to mechanical limitations of

Access this article online

Quick Response Code:

Website: www.jmp.org.in

DOI: 10.4103/jmp.jmp_176_23

Address for correspondence: Dr. Rose Kamal, Department of Radiation Oncology, Amrita Institute of Medical Sciences and Research Centre, Faridabad - 121 008, Haryana, India.
E-mail: rose.kamal22@gmail.com

How to cite this article: Kamal R, Thaper D, Singh G, Sharma S, Navjeet, Oinam AS, *et al*. Modeling of gamma index for prediction of pretreatment quality assurance in stereotactic body radiation therapy of the liver. J Med Phys 2024;49:232-9.

the delivery equipment and the dose calculation accuracy of the treatment planning system (TPS).[5] In this regard, patient-specific quality assurance (QA) is highly recommended to verify the plan delivery accuracy.[6] The gamma index is widely used for verification of either two-dimensional (2D) or 3D dose verification.[7,8] Derivative-based gamma has also been reported as a crucial pretreatment QA in addition to the conventional gamma for stereotactic treatment planning.[9] The use of linear accelerator (LINAC) treatment log files is also used for pretreatment QA.[10] However, these methods have both advantages and disadvantages.

Several previous studies have also demonstrated that the modulation complexity of the plan can be used to predict the deliverability (pretreatment QA) of a treatment plan as intended at the planning stage, and various parameters and formulas to evaluate the complexity of the plan have been reported.[4,11-17] Li and Xing reported a modulation complexity (MISPORT) based on the movements of the MLC weighted by a segmental monitor unit (MU) for VMAT.[11] Masi *et al*. proposed a leaf travel modulation complexity score and modulation complexity score for VMAT.[4] Du *et al*. studied many modulation indices for VMAT, including plan-averaged beam modulation, plan-averaged beam irregularity, plan-averaged beam area, and plan-normalized MU.[13] Park *et al*. suggested a modulation index (MI) that is based on the concept of Webb that incorporates MLC speed (LS), MLC acceleration, gantry acceleration, and DR for VMAT.[12,18] Park *et al*. also quoted the plan-averaged beam irregularity complexity measure as a predictor of IMRT plan delivery accuracy.[14]

Nicolini *et al*. demonstrated a robust compensation mechanism between gantry speed and DR in VMAT and concluded that the most dominant modulating parameter influencing the plan deliverability of the VMAT technique is the MLC movement.[16] A noteworthy study of 758 patients from various sites was reported, which made use of the MI calculated by Park *et al*. and incorporated the effects of jaw tracking and aperture area. It is quoted that gamma pass rates (GPRs) are more affected by conventional treatments by MLC modulation, while MU and jaw tracking affect the treatment deliverability in SABR.[17] Shen *et al*. reported that the MU, segment area, and planning target volume (PTV) size strongly affect the plan quality and deliverability of VMAT.[19] The degree of modulation (DoM) is also suggested as a measure of treatment plan complexity and considers the total MU delivered per unit fractional dose.[20] Another author compared the results of different TPS and concluded that TPS-specific parameters should be carefully selected to calculate MI for the prediction of plan deliverability.[21] Furthermore, the machine learning approach to predict the GPRs is reported with acceptable accuracy.[22-24]

None of the studies recommended a quantitative value and appropriate parameters to calculate the MI for its use as pretreatment QA specific to liver SBRT using Monaco TPS such that treatment delivery lies within a confidence interval. It is highly important in SBRT as the altered dose delivered due to a large MI may affect the mean liver dose, which is a critical constraint for liver SBRT. In this study, we presented a predictive model to evaluate pretreatment patient-specific QA based on treatment planning parameters for SBRT of liver carcinoma, which is easy to use, at the planning stage. The most profound parameters were rendered from several modulation indices available in the literature, such that minimal multicollinearity exists, using multivariate Least Absolute Shrinkage and Selection Operator (LASSO) analysis. Furthermore, the receiver operating curve (ROC) analysis of the model was performed.

Materials and Methods

Patient selection

One hundred and eighty patients with HCC were randomly selected for this retrospective study. All patients were positioned with BlueBAG™ (Elekta AB, Stockholm, Sweden) in the supine position. The patients underwent either four-dimensional or breath-hold or free-breathing 3D computed tomography (CT) scans, which were acquired using 64 Slice Optima GE CT equipment (GE Medical Systems, USA) integrated with a GE Discovery 710 time of flight positron emission tomography–CT scanner (GE Healthcare, Amersham, UK). A pressure sensor-based load cell device of the Anzai Gating System (AZ-733V; Anzai Medical System, Tokyo, Japan) using an elastic belt wrapped around the patient's abdomen was used for 4D and breath-hold scans to monitor the patient's respiratory waveform. An abdominal compression belt was used to restrict the motion of the free-breathing scans to reduce the internal target volume (ITV). To calculate the ITV, 4D scans were used. The slice thickness used for the patient scan was 2.5 mm. All structures were contoured as mentioned in the RTOG 1112 protocol.[25] The PTV was generated by providing a population-based 5 mm uniform margin around the ITV to incorporate setup uncertainties.

Treatment planning

All treatment plans were generated using Monaco TPS version 5.1 (Elekta CMS, Maryland Heights, MO, USA) for delivery with Versa HD (Elekta, Stockholm, Sweden) equipped with Agility MLC 80 leaf pairs for VMAT delivery, with a maximum DR of 600 MU/min using 10MV photon energy. Segment shape optimization with a minimum segment width of ~ 0.5 cm and medium fluence smoothing was used for the optimization of VMAT plans using the Monte Carlo dose calculation algorithm with a 2 mm grid size and 3% Monte Carlo variance. Treatment planning was performed with a very tight margin of 0–1 mm around the target using automatic jaw tracking. All patients were planned using two partial arcs (60°–180°; counter-clockwise and 180°–60°: clockwise) complementary collimator angles of 30° and 330° for prescription doses in the range of 4–10 Gy/fraction. The dose-volume constraints of PTV and organs at risk, as mentioned in RTOG 1112, were achieved.[25]

Modulation complexity indices

Various parameters that have been described in the literature, which predict the complexity of the treatment plans, were calculated, and are enumerated in Table 1. Few modulation indices were calculated using the formalism of Webb with a k-value of 0.5 sigma (MI_webb).[12,18,26] The resultant value was normalized to the total control points, except for the gantry travel, which was normalized to the total arc length. In addition, MCS_Masi, LT, LTMCS (Masi *et al*. 2013), and MISPORT (Li and Xing 2013) were calculated. The DICOM-RP file was exported and processed using an in-house algorithm written in MATLAB® software

Table 1: Modulation indices according to various parameters

	Formula
DoM[20]	$DoM = \frac{Total\ MU\ per\ fraction}{Dose\ per\ fraction\ in\ cGy}$
LT_MU_webb (MI_{LT})	$LT\_MU = \frac{leaf\ travel\ at\ each\ control\ point}{MU\ at\ each\ control\ point}$ $LT\_MU\_webb = \frac{MI\_webb\ (LT\_MU)}{total\ control\ points}$
JT_MU_webb (MI_{JT})	$JT\_MU = \frac{Jaw\ travel\ at\ each\ control\ point}{MU\ at\ each\ control\ point}$ $JT\_MU\_webb = \frac{MI\_webb\ (JT\_MU)}{total\ control\ points}$
GT_MU_webb (MI_{GT})	$GT\_MU = \frac{Gantry\ travel\ at\ each\ control\ point}{MU\ at\ each\ control\ point}$ $GT\_MU\_webb = \frac{MI\_webb\ (GT\_MU)}{total\ arc\ length}$
MUweightedArea_webb (MI_{MUWA})	$MUweightedArea = \frac{(segment\ MU \times segment\ area)}{totalMU}$ $MUweightedArea\_webb = MI\_webb\ (MUweightedArea)$
SegArea_MU_webb (MI_{SAMU})	$SegArea\_MU = \frac{Segment\ area\ at\ each\ control\ point}{MU\ at\ each\ control\ point}$ $SegArea\_MU\_webb = \frac{MI\_webb\ (SegArea\_MU)}{total\ control\ points}$
segmentMU_webb (MI_{MU})	$segmentMU\_webb = \frac{MI\_webb\ (segment\ MU)}{total\ control\ points}$
segmentarea_webb (MI_{SA})	$segmentarea\_webb = \frac{MI\_webb\ (segment\ area)}{total\ control\ points}$
AAV_CP_Masi_webb[4] (MI_{AAV})	$AAV\_CP\_Masi\_webb = \frac{MI\_webb\ (AAV\_CP\_Masi)}{total\ control\ points}$
LSV_CP_Masi_webb[4] (MI_{LSV})	$LSV\_CP\_Masi\_webb = \frac{MI\_webb\ (LSV\_CP\_Masi)}{total\ control\ points}$
DR_webb[12,16] (MI_{DR})	$DR\_webb = \frac{MI\_webb\ (DR)}{total\ control\ points}$
LS_webb[12,16] (MI_{LS})	$LS\_webb = \frac{MI\_webb\ (LS)}{total\ control\ points}$
GS_webb[12,16] (MI_{GS})	$GS\_webb = \frac{MI\_webb\ (GS)}{total\ control\ points}$
JS_webb[12,16] (MI_{JS})	$JS\_webb = \frac{MI\_webb\ (JS)}{total\ control\ points}$

DR: Dose rate, DoM: Degree of modulation, GS: Gantry speed, LS: Leaf speed, MI: Modulation index, MU: Monitor unit

version R2011b (MathWorks, Natick, MA) to calculate the modulation indices.

Patient-specific QA measurement

The gamma evaluation method was used as a measure of the VMAT plan delivery accuracy. An Octavius 1500™ (PTW, Freiburg, Germany) detector array tandem with a cavity was placed on the treatment table for the measurement. The array consists of 1405 chambers that were mounted below a 0.5 cm polystyrene build-up layer, and the spacing between the centers of two adjacent chambers was 7.1 mm.[27] The Octavius CT-IC (PTW, Freiburg, Germany) with a 2D array was used for CT scan acquisition and dose calculation.[28] The verification plans for gamma evaluations were calculated with a calculation grid of 2 mm and 3% statistical variation using the Monte Carlo method in Monaco TPS. The array was always cross-calibrated with the phantom for 2 Gy at the level of the effective point of measurement of the array (isocenter) in water equivalent reference conditions corresponding to 10 cm × 10 cm. Two array measurements were always taken for the same plan with one measurement using the array center positioned at the plan isocenter and the other measurement by shifting the couch by 5 mm superiorly. Both measurements were then merged to determine the final measured fluence, resulting in a comparatively higher spatial resolution of 5 mm.

The Verisoft software (version 7.1, PTW, Freiburg, Germany) was used to calculate the global gamma index with gamma criteria of 2%/2 mm and 3%/3 mm. Pixels with a dose value >10% of the maximum dose were evaluated with an increased tolerance of 10% dose difference for values below 0.3.[29] The center of the dose matrix was chosen as the normalization point. The calculated dose distribution was aligned with the origin of the measured dose matrix. For each patient, the ROI was defined to cover the target as well as the low-dose area. The analysis performed was always in a relative mode such that the dose at the isocenter for the measured and calculated distributions was the same.

Statistical analysis and data validation

All statistical analyses were performed using the SPSS Statistics for Windows (version 20.0. IBM Corporation, Armonk, NY) and STATA for Windows (version 16, StataCorp, Texas, USA). The GPR is a variable dependent on the modulation complexity parameters. The mean and standard deviation of the modulation indices, PTV size, and the GPRs were calculated. The LASSO regression analysis was performed to derive a predictive linear model as it removes the redundant data to minimize multicollinearity. Double cross-validation (10-fold) was executed on the training dataset extracted from the total dataset to test the accuracy of prediction.[30] The multicollinearity of the data was tested using the variance inflation factor (VIF < 5). The sensitivity and specificity of the model were also analyzed using ROC curves. The mean, standard deviation, root mean square error (RMSE), and mean absolute error (MAE) were calculated for the validation dataset of 10 new routine patients to evaluate the performance of the model.[22]

Results

Modulation complexity indices

The statistical analysis (range, average, and standard deviation) of various MIs, PTV size, as well as GPRs of global gamma evaluation with gamma criteria of 2%/2 mm (G22) and 3%/3 mm (G33) used in this study is shown in Table 2.

The correlation analysis between MIs, PTV size, and global GPRs with gamma criterion of 2%/2 mm and 3%/3 mm is shown in Table 3. Spearman's correlation coefficient (r_s) was calculated along with the *P* value. MI_{LS} and PTV size showed the highest correlation with both the gamma criteria of 2%/2 mm and 3%/3 mm. The r_s values of MI_{LS} with G22 and G33 were −0.407 and −0.351, respectively, with $P < 0.01$, whereas the r_s values of PTV size with G22 and G33 were −0.455 and −0.411, respectively, with $P < 0.01$.

Table 4 presents the VIF values of the modulation indices used in the multivariate model to predict the GPRs. The VIF values of all the parameters were <2, which indicates that these data were weakly associated with each other.[31] The coefficients, intercept, and R-squared value for the model are calculated for the prediction of global GPRs with a global gamma criterion of 2%/2 mm and 3%/3 mm as shown in Table 5. For G22 prediction, DoM, MCS_{SPORT}, gantry speed (MI_{GS}), and leaf speed (MI_{LS}) were predictive variables, whereas for G33 prediction,

Table 2: Quantitative analysis of modulation indices (mean, range, and standard deviation)

	Range	Average	SD
DoM	1.824–9.824	5.014	1.578
MCS_{Masi}	0.039–0.397	0.120	0.048
MCS_{SPORT}	993.719–56,185.692	10,726.873	7379.763
MCS_LT	54.378–322.396	156.202	50.167
LTMCS	0.032–0.374	0.102	0.044
MI_{LT}	1.059–26.324	9.914	5.149
MI_{JT}	0.123–1.304	0.515	0.240
MI_{GT}	0.043–0.350	0.189	0.070
MI_{MUWA}	2.656–32.111	12.974	5.495
MI_{SAMU}	0.855–9.364	3.158	1.629
MI_{MU}	0.404–24.347	5.565	3.530
MI_{SA}	1.271–11.182	4.568	1.815
MI_{AAV}	0.0082–0.096	0.026	0.012
MI_{LSV}	0.013–0.074	0.036	0.011
MI_{DR}	6.989–138.728	70.708	29.292
MI_{LS}	9.767–120.748	41.558	21.403
MI_{GS}	0.420–2.031	1.210	0.267
MI_{JS}	0.680–4.462	2.307	0.747
RDM	106.77–926.02	270.09	101.881
PTV size	73.00–3193.00	799.29	647.39
G22 (2%/2 mm)	61.30	76.139	11.468
G33 (3%/3 mm)	28.20	92.198	6.464

SD: Standard deviation, DoM: Degree of modulation, PTV: Planning target volume, GS: Gantry speed, LS: Leaf speed, MI: Modulation index, MU: Monitor unit, MCS: Modulation complexity score, RDM: Relative degree of modulation, LTMCS: Leaf travel modulation complexity score

DoM, MCS_{SPORT}, Robust decision making (RDM), and leaf speed (MI_{LS}) are important predictors, as shown in Table 5.

The indices to assess the reliability of the predictive model, such as MAE and RMSE, calculated for 10 new routine patients of SBRT liver, are presented in Table 6. The sensitivity and specificity of the predictive model were evaluated, and the results for G22 and G33 are shown in Table 7. Two ROC curves were generated corresponding to the G22 and G33 criteria [Figure 1]. The process-based threshold (reference value) was calculated from the measured data as recommended in TG-218.[32] A threshold for the predictive model was then selected from ROC curves where the sum of specificity and sensitivity is near to one.[33]

Table 3: Correlation analysis between global gamma passing rates with various gamma criteria and the modulation indices for volumetric modulated arc therapy plans

MI	2%/2 mm		3%/3 mm	
	r_s	*P*	r_s	*P*
DoM	−0.287	<0.01	−0.275	<0.01
MCS_Masi	0.177	0.014	0.211	<0.01
MCS_SPORT	−0.339	<0.01	−0.317	<0.01
MCS_LT	−0.248	<0.01	−0.223	<0.01
LTMCS	0.212	<0.01	0.237	<0.01
MI_{LT}	−0.311	<0.01	−0.291	<0.01
MI_{JT}	−0.163	0.025	−0.183	0.012
MI_{GT}	0.110	0.131	0.103	0.157
MI_{MUWA}	−0.310	<0.01	−0.253	<0.01
MI_{SAMU}	−0.225	<0.01	−0.182	0.012
MI_{MU}	0.02	0.786	−0.002	0.978
MI_{SA}	−0.264	<0.01	−0.228	<0.01
MI_{AAV}	0.335	<0.01	0.343	<0.01
MI_{LSV}	0.341	<0.01	0.332	<0.01
MI_{DR}	0.093	0.2	0.083	0.252
MI_{LS}	−0.407	<0.01	−0.351	<0.01
MI_{GS}	0.079	0.280	0.123	0.090
MI_{JS}	−0.351	<0.01	−0.313	<0.01
PTV size	−0.455	<0.01	−0.411	<0.01

DoM: Degree of modulation, PTV: Planning target volume, GS: Gantry speed, LS: Leaf speed, MI: Modulation index, MU: Monitor unit, MCS: Modulation complexity score, LTMCS: Leaf travel modulation complexity score

Table 4: Variance inflation factor among modulation index obtained for the predictive model (1) using 2%/2 mm gamma criteria (2) using 3%/3 mm gamma criteria

GC	DoM	MCS_{SPORT}	MI_{LS}	MI_{GS}	RDM
G22	1.179	1.741	1.575	1.056	-
G33	1.412	2.071	1.588	-	1.312

DoM: Degree of modulation, GS: Gantry speed, LS: Leaf speed, MI: Modulation index, MCS: Modulation complexity score, RDM: Relative degree of modulation

Discussion

The use of modulation complexity as a pretreatment QA has been studied by many authors. Higher modulation in VMAT plans increases the differences between the planned and measured dose distributions (pretreatment QA results). Different authors have used different modulation indices to predict plan deliverability and showed correlations with GPRs. However, none of the authors compared the effectiveness of the parameters used for the calculation of MI to predict the GPRs. Furthermore, the models were not handy to use in routine clinics.

In this study, we designed a predictive model to use MI as a pretreatment QA for liver SBRT cases using multivariate regression. The various parameters [Table 1] that may affect the modulation and hence the uncertainty of the treatment plan were calculated from the DICOM-RP file of the patient. However, few of these parameters have a high underlying association and correlation. Thus, all the extracted parameters were not redundant. We extracted a few nonredundant parameters that could be used to predict the GPRs. The formalism of Webb was used to calculate the modulation indices because it adds weight on variations larger than a certain threshold value, in contrast to conventional methods, which is simply the average of the data.[18] As the impact of larger variations is potentially greater, the formalism of Webb may show better performance.

In previous studies, few MIs were checked for correlation with GPRs using the Spearman correlation analysis with statistical significance. MCS_v and MI_{SPORT} showed a positive correlation, which agreed with the results of Park *et al*., in 2014. The results of MI_{DR} ($P > 0.05$) and MI_{LS} ($P < 0.01$) in the present study are similar to that found in the study of Park *et al*., in 2014. This can be attributed to the fact that different TPS were used in the two studies. As suggested, one parameter that affects the plan complexity in one TPS may have an insignificant effect on modulation in another TPS.[21]

Since 2%/2 mm and 3%/3 mm evaluate the plan deliverability, we have presented two models corresponding to 3%/3 mm and 2%/2 mm global gamma evaluation criterion.[29] Brushi *et al*. studied the effect of the resolution of an array on the evaluation of GPRs and showed reasonable accuracy of the measured dose distribution of the Octavius 1500 module (merged from two

Table 5: The regression coefficients for various modulation index parameters intercept values obtained using a predictive model for (a) equation number 1 using 2%/2 mm gamma criteria (b) equation number 2 using 3%/3 mm gamma criteria

GC	Coff_DoM (a)	Coff_MCS_{SPORT} (b)	Coff_MI_{LS} (c)	Coff_MI_{GS} (d)	RDM (e)	Intercept (*f*)	R^2
G22	−0.492	−0.0000553	−0.0569	1.4456	-	99.30	0.2625
G33	−0.08968	−0.0000376	−0.014291	-	−0.0017559	101.1919	0.2082

DoM: Degree of modulation, GS: Gantry speed, LS: Leaf speed, MI: Modulation index, MCS: Modulation complexity score, RDM: Relative degree of modulation

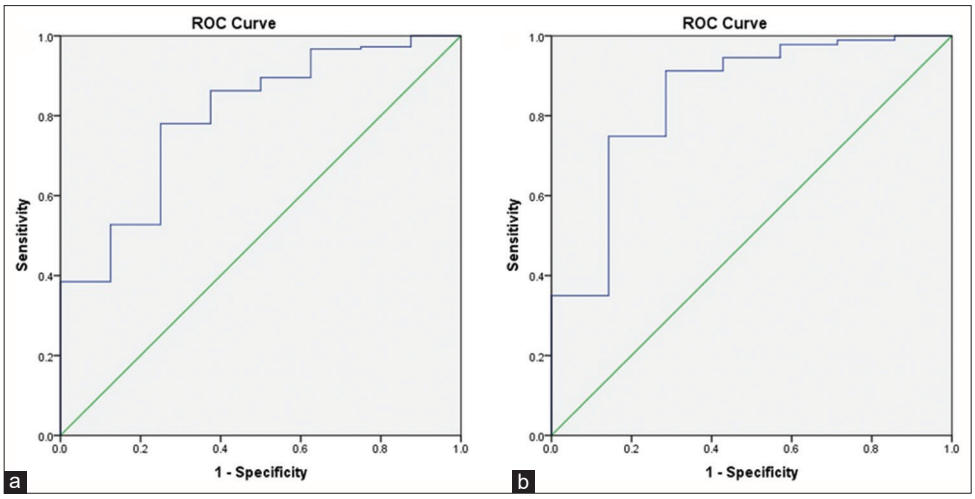

Figure 1: Receiver operating curve analysis (a) G22, (b) G33

Table 6: Comparative indices obtained for the predictive model for new 10 patients (1) for 2%/2 mm gamma criteria (2) for 3%/3 mm gamma criteria

GC prediction model	Mean±SD	MAE	RMSE
G22	0.91±3.39	2.33	3.07
G33	0.21±1.19	0.72	1.14

SD: Standard deviation, MAE: Mean absolute error, RMSE: Root mean square error

Table 7: Sensitivity and specificity analysis of predictive model for various global gamma criteria

GC	Sensitivity (%)	Specificity (%)	Threshold (%)	AUC
G22	75	75	94.6	0.801
G33	74.9	85.7	98.9	0.846

AUC: Area under curve

measurements) for gamma evaluation.[34] Using the LASSO method of predictor selection in multivariate regression, only those variables are extracted such that variables are minimally multicollinear (VIF <5).

In addition, the pretreatment QA devices and LINAC used in this study are different from those used in the previous study. The MI_{LS} and PTV size showed the highest correlation with the GPRs ($P < 0.05$). The present model includes various factors that can affect uncertainty in treatment delivery. The noncollinear factors with statistical significance were extracted to derive the model. In theory, the performance of the model should be superior to that of other published modulation indices, as not all the parameters that may affect the complexity of the plan were included. In addition, the factors that affect treatment delivery were quoted. The model suggests that DoM, MCS_{SPORT}, gantry speed (MI_{GS}), and leaf speed (MI_{LS}) affect the plan delivery accuracy, the highest in SBRT cases being that for the 2%/2 mm cases, whereas, DoM, MCS_{SPORT}, RDM, and leaf speed (MI_{LS}) affected the plan deliverability by 3%/3 mm. These indices are extracted from statistical analysis where VIF <2, suggesting weak correlation/multicollinearity exists between these parameters as shown in Table 4. VIF (inversely proportional to [1– R^2]) quantifies the extent to which multicollinearity increases the variance of an estimated regression coefficient. The linearly independent variables correspond to $R^2 = 0$ and VIF = 1. Thus, some parameters that are significantly correlated with the results of pretreatment QA pass rates were identified. The coefficients of the dependent parameters of the empirical formula were found to predict the GPRs for various gamma criteria as shown in Table 5. To evaluate predictive model performance, the calculated mean ± standard deviation (%), MAE, and RMSE were evaluated in one study for the validation dataset, and the corresponding results were −0.2 ± 4.2, 3.2%, and 4.2%, respectively, for G22 gamma evaluation criteria.[22] The obtained values in our study were comparable to this study as shown in Table 6.

By plotting the trade-off between sensitivity and specificity, ROC curves provide a comprehensive view of the predictive model and identify the selection of an appropriate threshold for making classification decisions. As shown in Figure 1 and Table 7, the specificity and sensitivity for the G22 prediction model were 75.0% and 75.0% for the threshold of 94.6% GPR, respectively, whereas the corresponding values for the G33 prediction were 85.7% and 74.9% for the threshold of 98.9% GPR, respectively. For the implication of the predictive model on new patients, if results for G22 and G33 are more than threshold values of 94.6% and 98.9%, respectively, then it can be considered as passed for pretreatment patient-specific QA. The classification process with a predictive model helps to decide "pass" or "fail," as a clinical decision-making system. The sensitivity of the model would be imperative to determine the effect on delivery accuracy. The area under the curve (AUC) in the ROC curves is the measurement of model performance. The AUC of G22 and G33 was 0.801 and 0.846, respectively. The AUC value of more than 0.7 suggests the better overall performance of the model across all possible thresholds.[33]

The machine learning approach used in literature to predict GPRs is quite complex to use for planners as it requires thorough knowledge and expertise to develop and use the software. The model derived here gives an empirical formula that is quite handy and easy to use in routine practice and is accurate at an acceptable level. Although gamma analysis is a measure of potential deviations from the planned dose, its resolution and dose calculation uncertainty of TPS can also affect its results. In addition, planar measurements and 2D gamma analysis were performed in the present study. By contrast, a more sophisticated approach of 3D gamma analysis could be used for volumetric results. This will be investigated in future work using a large dataset of VMAT plans. Another limitation of the study is that we were unable to extract the actual delivered parameters from log files of Elekta to evaluate whether higher modulation results in deviations of planned parameters, could result in a significant change in dose-volume parameters. In addition, various QA systems will be investigated in further studies. The derivative-based gamma approach is reported to be useful for stringent patient-specific QA for SBRT of the liver and will be studied in future works. The present study was conducted for one site along with a specific QA system and treatment delivery machine. A randomized multi-institutional study for multiple sites and various systems is required to generate a generalized predictive model.

Conclusions

This study aimed to develop a predictive model to calculate GPRs by focusing on the DoM using multivariate LASSO regression analysis. DoM, MCS_{SPORT}, gantry speed (MI_{GS}), and leaf speed (MI_{LS}) were found to be predictors of global GPRs for 2%/2 mm, whereas DoM, MCS_{SPORT}, RDM, and leaf speed (MI_{LS}) were predictors of the global gamma criterion of 3%/3 mm. The model is potentially beneficial as an alternative to pretreatment QA in predicting the uncertainty in plan deliverability at the planning stage and thus can reduce resources in busy clinics. This would lead to efficient and rapid decision-making for determining plan quality, especially in online adaptive radiotherapy planning, these mathematical predictive models would facilitate the clinical decisions.

Financial support and sponsorship

Nil

Conflicts of interest

There are no conflicts of interest.

References

1. Mahadevan A, Blanck O, Lanciano R, Peddada A, Sundararaman S, D'Ambrosio D, *et al*. Stereotactic body radiotherapy (SBRT) for liver metastasis – Clinical outcomes from the international multi-institutional RSSearch® patient registry. Radiat Oncol 2018;13:26.
2. Thaper D, Kamal R, Singh G, Oinam AS, Yadav HP, Kumar R, *et al*. Dosimetric comparison of dynamic conformal arc integrated with segment shape optimization and variable dose rate versus volumetric modulated arc therapy for liver SBRT. Rep Pract Oncol Radiother 2020;25:667-77.
3. Otto K. Volumetric modulated arc therapy: IMRT in a single gantry arc. Med Phys 2008;35:310-7.
4. Masi L, Doro R, Favuzza V, Cipressi S, Livi L. Impact of plan parameters on the dosimetric accuracy of volumetric modulated arc therapy. Med Phys 2013;40(7):071718.
5. Giorgia N, Antonella F, Eugenio V, Alessandro C, Filippo A, Luca C. What is an acceptably smoothed fluence? Dosimetric and delivery considerations for dynamic sliding window IMRT. Radiat Oncol 2007;2:42.
6. Measurements IC on RU and. Prescribing, Recording, and Reporting Intensity-Modulated Photon-Beam Therapy (IMRT)(ICRU Report 83); 2010.
7. Low DA, Harms WB, Mutic S, Purdy JA. A technique for the quantitative evaluation of dose distributions. Med Phys 1998;25:656-61.
8. Wendling M, Zijp LJ, McDermott LN, Smit EJ, Sonke JJ, Mijnheer BJ, *et al*. A fast algorithm for gamma evaluation in 3D. Med Phys 2007;34:1647-54.
9. Thaper D, Kamal R, Singh G, Oinam AS, Yadav HP, Kumar V. Derivative-based gamma index: A novel methodology for stringent patient-specific quality assurance in the stereotactic treatment planning of liver cancer. Biomed Phys Eng Express 2020 Sep 29;6(6). [doi: 10.1088/2057-1976/ababf3].
10. Schreibmann E, Dhabaan A, Elder E, Fox T. Patient-specific quality assurance method for VMAT treatment delivery. Med Phys 2009;36:4530-5.
11. Li R, Xing L. An adaptive planning strategy for station parameter optimized radiation therapy (SPORT): Segmentally boosted VMAT. Med Phys 2013;40:050701.
12. Park JM, Park SY, Kim H, Kim JH, Carlson J, Ye SJ. Modulation indices for volumetric modulated arc therapy. Phys Med Biol 2014;59:7315-40.
13. Du W, Cho SH, Zhang X, Hoffman KE, Kudchadker RJ. Quantification of beam complexity in intensity-modulated radiation therapy treatment plans. Med Phys 2014;41:021716.
14. Park SY, Kim JI, Chun M, Ahn H, Park JM. Assessment of the modulation degrees of intensity-modulated radiation therapy plans. Radiat Oncol 2018;13:244.
15. Park JM, Kim JI, Park SY. Modulation indices and plan delivery accuracy of volumetric modulated arc therapy. J Appl Clin Med Phys 2019;20:12-22.
16. Nicolini G, Clivio A, Cozzi L, Fogliata A, Vanetti E. On the impact of dose rate variation upon RapidArc implementation of volumetric modulated are therapy. Med Phys 2011;38:264-71.
17. Chun M, Joon An H, Kwon O, Oh DH, Park JM, Kim JI. Impact of plan parameters and modulation indices on patient-specific QA results for standard and stereotactic VMAT. Phys Med 2019;62:83-94.
18. Webb S. Use of a quantitative index of beam modulation to characterize dose conformality: Illustration by a comparison of full beamlet IMRT, few-segment IMRT (fsIMRT) and conformal unmodulated radiotherapy. Phys Med Biol 2003;48:2051-62.
19. Shen L, Chen S, Zhu X, Han C, Zheng X, Deng Z, *et al*. Multidimensional correlation among plan complexity, quality and deliverability parameters for volumetric-modulated arc therapy using canonical correlation analysis. J Radiat Res 2018;59:207-15.
20. Hubley E, Pierce G. The influence of plan modulation on the interplay effect in VMAT liver SBRT treatments. Phys Med 2017;40:115-21.
21. Hernandez V, Saez J, Pasler M, Jurado-Bruggeman D, Jornet N. Comparison of complexity metrics for multi-institutional evaluations of treatment plans in radiotherapy. Phys Imaging Radiat Oncol 2018;5:37-43.
22. Hirashima H, Ono T, Nakamura M, Miyabe Y, Mukumoto N, Iramina H, *et al.* Improvement of prediction and classification performance for gamma passing rate by using plan complexity and dosiomics features. Radiother Oncol 2020;153:250-7.
23. Ono T, Hirashima H, Iramina H, Mukumoto N, Miyabe Y, Nakamura M, *et al.* Prediction of dosimetric accuracy for VMAT plans using plan complexity parameters via machine learning. Med Phys 2019;46:3823-32.

24. Tomori S, Kadoya N, Kajikawa T, Kimura Y, Narazaki K, Ochi T, *et al.* Systematic method for a deep learning-based prediction model for gamma evaluation in patient-specific quality assurance of volumetric modulated arc therapy. Med Phys 2021;48:1003-18.
25. Dawson L, Zhu A, Knox J, Krishnan S, Craig T, Guha C*, et al*. Radiation Therapy Oncology Group Rtog 1112 Randomized Phase iii Study of Sorafenib Versus Stereotactic Body Radiation Therapy followed by Sorafenib in Hepatocellular Carcinoma; 2013.
26. Boylan CJ, Rowbottom CG, Mackay RI. The use of a realistic VMAT delivery emulator to optimize dynamic machine parameters for improved treatment efficiency. Phys Med Biol 2011;56:4119-33.
27. Van Esch A, Basta K, Evrard M, Ghislain M, Sergent F, Huyskens DP. The Octavius1500 2D ion chamber array and its associated phantoms: Dosimetric characterization of a new prototype. Med Phys 2014;41(9).
28. Van Esch A, Clermont C, Devillers M, Iori M, Huyskens DP. On-line quality assurance of rotational radiotherapy treatment delivery by means of a 2D ion chamber array and the octavius phantom. Med Phys 2007;34:3825-37.
29. Kim JI, Park SY, Kim HJ, Kim JH, Ye SJ, Park JM. The sensitivity of gamma-index method to the positioning errors of high-definition MLC in patient-specific VMAT QA for SBRT. Radiat Oncol 2014;9:167.
30. Lee TF, Chao PJ, Ting HM, Chang L, Huang YJ, Wu JM, *et al.* Using multivariate regression model with least absolute shrinkage and selection operator (LASSO) to predict the incidence of xerostomia after intensity-modulated radiotherapy for head and neck cancer. PLoS One 2014;9:e89700.
31. Reddy MC, Balasubramanyam DP, Subbarayudu PM. An effective approach to resolve multicollinearity in agriculture data. IJRECE 2013;1:2348-2281.
32. Miften M, Olch A, Mihailidis D, Moran J, Pawlicki T, Molineu A, *et al.* Tolerance limits and methodologies for IMRT measurement-based verification QA: Recommendations of AAPM task group no. 218. Med Phys 2018;45:e53-83.
33. Nahm FS. Receiver operating characteristic curve: Overview and practical use for clinicians. Korean J Anesthesiol 2022;75:25-36.
34. Bruschi A, Esposito M, Pini S, Ghirelli A, Zatelli G, Russo S. How the detector resolution affects the clinical significance of SBRT pre-treatment quality assurance results. Phys Med 2018;49:129-34.